Multichroic seashell antenna with internal filters by resonant slots and cold-electron bolometers

(article starts on next page)

Multichroic seashell antenna with internal filters by resonant slots and cold-electron bolometers

L S Kuzmin[1,2] , **A V Blagodatkin**[2,3], **A S Mukhin**[1,2], **D A Pimanov**[2],
V O Zbrozhek[2], **A V Gordeeva**[2,3], **A L Pankratov**[2,3] and **A V Chiginev**[2,3]

[1] Chalmers University of Technology, Gothenburg SE-41296, Sweden
[2] Nizhny Novgorod State Technical University n.a. R.E. Alekseev, Nizhny Novgorod 603951, Russia
[3] Institute for Physics of Microstructures, Russian Academy of Sciences, Nizhny Novgorod 603950, Russia

E-mail: kuzmin@chalmers.se

CrossMark

Abstract

We have developed and realized a novel multichroic seashell antenna with internal bandpass filters by resonant slots and cold-electron bolometers (CEB). Slots and CEBs are connected by coplanar waveguides (CPW) instead of microstrip lines to realize the most reliable single-layer technology. The internal resonance is organized by a series resonance of slots with CPW and capacitances of superconductor/insulator/normal (SIN) tunnel junctions. In contrast, a conventional multichroic pixel consists of a wideband sinuous antenna coupled to TES detectors by long microstrip lines with overlap and external on-chip filters for different frequency bands. A common problem with a conventional multichroic pixel is that the beam width is frequency dependent for different frequency bands. Besides that, this system with external filters is quite large and includes long microstrip lines with unavoidable overlap and rater high losses. The multichroic seashell antenna with internal resonances avoids all these problems. The main advantage of this antenna is an opportunity to tune separate pairs of phased slots for each frequency band independently. We used pairs of $\lambda/2$ slots for 75 and 105 GHz, connected by CPW to CEBs. The connection of CPW to slots was shifted closer to the end of slots for proper RF matching. Each CEB included two SIN junctions and an absorber. SIN junctions had capacitances of 77 and 67 fF. Wave impedance of the antenna was near 50 Ohm and resistance of the absorber was matched to this value. RF testing was done at 314 mK irradiating this chip by frequency sweep of a generator from 78–118 GHz. The response curves have shown clear resonances around 75 and 105 GHz with a quality factor around 5. These experiments confirmed that the seashell antenna with the internal filters by resonant slots and CEBs could effectively be used for creating multiband elements.

Keywords: SIN tunnel junctions, cold-electron bolometer, seashell slot antenna, multichroic pixel, bandpass filters

(Some figures may appear in colour only in the online journal)

1. Introduction

Measurements of the cosmic microwave background (CMB) anisotropies will test models of inflationary cosmology, as well as other cosmological parameters [1]. The low intensity of the B-mode signal combined with the need to remove polarized galactic foregrounds requires an extremely sensitive

millimeter receiver and effective methods of foreground removal. Current bolometric detector technology is reaching the limit set by the CMB photon noise. Thus, we need to increase the optical throughput to increase an experiment's sensitivity. To increase the throughput without increasing the focal plane size, we can increase the frequency coverage of each pixel. Increased frequency coverage per pixel has the additional advantage that the signal can be split into frequency bands to obtain spectral information. The detection of multiple frequency bands allows for removal of the polarized foreground emission from synchrotron radiation and thermal dust emission, by utilizing its spectral dependence. Traditionally, spectral information has been captured with a multichroic focal plane consisting of a heterogeneous mix of single-color pixels. To maximize the efficiency of the focal plane area, we need to develop a multichroic pixel [2]. This increases the number of pixels per frequency, at no extra cost per focal plane area, weight and cryogenic cost.

This paper is in the scope of the European Space Agency Technical Research Programme (TRP) investigating alternative architectures for focal plane configurations suitable for future space missions to detect the B-mode component of the CMB anisotropy [3]. In this programme, we are trying to develop relevant technology to replace the traditional corrugated horn antennas by planar antennas and create multichroic pixels. This work is relevant to development of technology for proposed missions such as COrE (Cosmic Origins Explorer). We propose a technology with dual frequency operation but in principle, the pixel should operate over more potential channels. Introducing multichroic operation means that the focal plane pixel number can be reduced by combining the traditional single frequency pixel into a multichroic pixel.

The cold-electron bolometers (CEBs) [4–6], based on self-cooling by superconductor/insulator/normal (SIN) tunnel junctions, are promising detectors for various space missions and balloon telescopes due to their unique properties, such as high sensitivity and wide dynamic range (due to the electron cooling effect). Another key advantage of CEBs is their insensitivity to cosmic rays due to the tiny volume of the absorber and decoupling of the phonon and electron subsystems [7].

Since bolometers are broadband detectors, certain LC filters, restricting the required frequency band, are needed. In case of geometric inductance, the size of such filters is rather large and comparable with a wavelength [2]. However, another key advantage of CEBs is their micron size, allowing to place them inside an antenna without long transmission lines leading to additional losses. With the use of large external filters, such advantage of CEBs would be lost.

The first breakthrough in realization of nanofilter was invention of CEBs with kinetic inductance of NbN strip [8]. The resonance was realized by capacitance of SIN tunnel junction and the kinetic inductance of NbN strip embedded into a cross slot antenna. The solution of this problem is based on the use of the kinetic inductance of the superconductor, allowing to reduce linear size of such an inductor up to 300 times compared to the geometrical inductor of the same

inductance. This strip is unified with a CEB and called a resonant cold-electron bolometer (RCEB).

The RCEB for multichroic pixels with an internal resonance by a kinetic inductance of the NbN nanostrip and a capacitance of the SIN tunnel junctions has been realized using a single Lambda slot with two RCEBs for 75 and 105 GHz [9]. However, the fabrication of kinetic inductance meets serious technological difficulties.

In the present paper, we suggest an alternative solution for creating multichroic system using internal resonance of slot antenna and capacitance of CEBs.

2. Multichroic seashell antenna with internal filters by resonant slots and CEBs

As an inductive element of a resonant circuit for matching with the capacitance of CEBs, we suggest the use of the reactance of the 'slot antenna + coplanar line' system. This approach implies that the imaginary part of the impedance of this reactance is positive at the operation frequency, which corresponds to the inductive character of such a system.

As the prototype of the receiving system we have chosen a COrE two-frequency single pixel at 75 and 105 GHz. This pixel is based on the two-frequency seashell antenna, which consists of pair of slot antennas connected with CEBs by coplanar lines [10].

This seashell antenna has several advantages. The main advantage is that slots for both frequencies are located in one pixel. This arrangement can solve the problem of aberrations and uniformity of the beam pattern across the entire focal plane. Further, each frequency channel of this antenna can be tuned independently including frequency bandwidth and beam width. Besides, this antenna can solve the problem with the optimal pixel size which arises from the dependence of beam width on frequency [11]. As the seashell antenna consists of several independent combinations of slot antennas, the distance between slots can be chosen to be optimal in each frequency channel.

In this paper, we consider a pixel for one polarization of the incoming signal, assuming that the system for two perpendicular polarizations will be studied later. The sample contains nine single pixel cells with two bands of 75 and 105 GHz and RLC-circuit, which determines the frequency selectivity of the receiving system. As a result, samples of frequency-selective receiving systems were fabricated and measured for two frequencies without the kinetic inductance of NbN strip. Instead of the NbN kinetic inductance, the total reactance of the coplanar line and slot antenna is used in the resonant circuit. The receiving system has bandpass filters at frequencies of 75 and 105 GHz.

3. Numerical modelling of the seashell antenna with CEBs

The design of the two-frequency seashell antenna for 75 and 105 GHz and one polarization is shown in figure 1. The
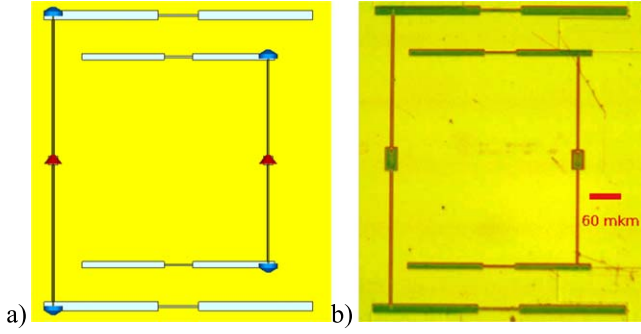
Figure 1. The design of the multichroic two-frequency seashell antenna for one polarization. (a) A view of the design in CST Microwave Studio; (b) optical photo of the fabricated antenna system of the sample.

antenna consists of two pairs of slots separated by $\lambda/2$ to form the required beam characteristics. The slot antennas are connected to CEBs by coplanar lines, and CEB is inserted into the gap in the central wire of the coplanar. The positions of CEBs are shown by red triangles in figure 1. Such a connection provides operation of the phased slots providing thus the needed radiation diagram of the antenna.

In the present design, to connect CEB with the slots, we have decided to use coplanar lines instead of microstrip lines. This solution has several advantages. The most important is that the design with coplanar lines requires less number of layers (one layer instead of three layers) and the technological process of fabrication of such a structure is dramatically simplified.

The DC biasing of CEB is provided through coplanar lines by DC connectors, which are located under the ground plane. The positions of DC connectors are shown by blue triangles in figure 1(a). In the modeling, the influence of the DC connectors on the electrodynamics of the antenna is taken into account by the effective capacitances of the connectors, which are connected between coplanars and ground plane and have the value of 200 fF. The optical photo of the fabricated antenna system with CEBs is shown in figure 1(b).

The numerical modeling of the two-frequency seashell antenna is performed in CST Microwave Studio. The electrodynamical part of the calculations is made by two solvers —time domain and frequency domain. The comparison of the results obtained by these two solvers demonstrates their similarity.

Figure 2 shows the real and imaginary parts of the antenna impedance vs frequency. From the electrodynamical part of calculations, we obtain the values of diagonal components of the Z-matrix at operating frequencies 75 and 105 GHz. Here $ReZ_{11}(75 \text{ GHz}) = 54.1 \text{ Ohm}$, $ImZ_{11}(75 \text{ GHz}) = 27.8 \text{ Ohm}$, $ReZ_{22}(105 \text{ GHz}) = 43.7 \text{ Ohm}$, and $ImZ_{22}(105 \text{ GHz}) = 22.7 \text{ Ohm}$. We use these values to obtain required resonances at operating frequencies in schematics.

Further, we have performed the modeling of the seashell antenna with schematics, based on previously made calculations in electrodynamics. The equivalent circuit of CEB connected to a seashell antenna (figure 3(a)) is an RC circuit,
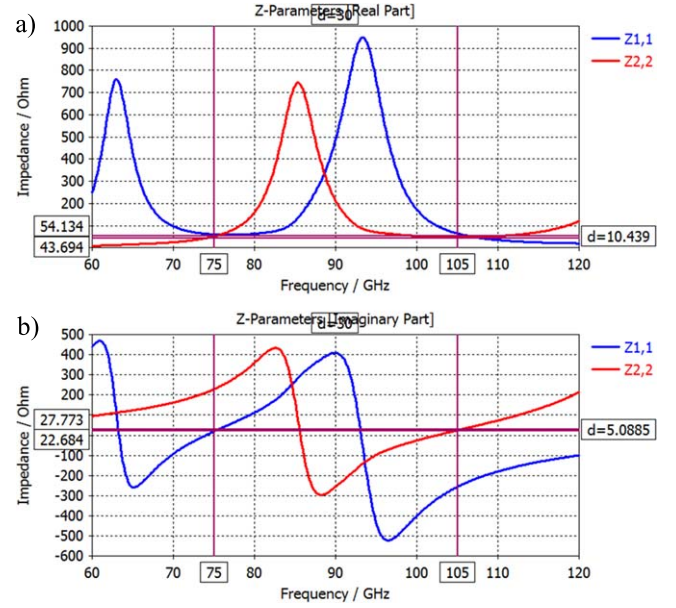

Figure 2. (a) ReZ and (b) ImZ of the seashell antenna versus frequency for 75 GHz (blue) and 105 GHz (red) channels.
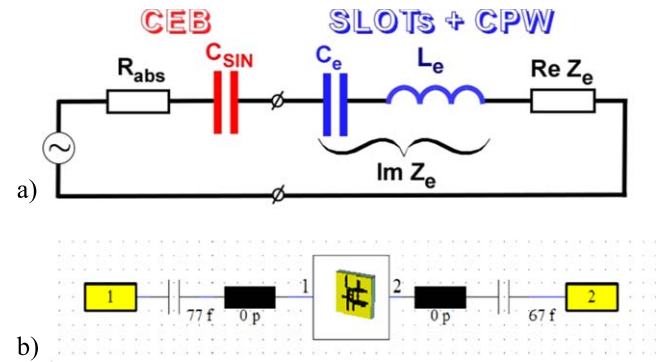

Figure 3. (a) Equivalent circuit of the seashell antenna connected with a CEB, (b) the equivalent circuit used in the numerical modeling.

where the resistance of a port corresponds to the resistivity of the CEB absorber R_{abs}, and the capacitance corresponds to the total capacitances of two SIN junctions of the CEB connected in series C_{SIN}. The inductance in this circuit is set to 0, as we consider the case of the CEB without an NbN strip. The equivalent curcuit of the seashell antenna with coplanar waveguides (CPW) consists of the capacitance C_e, inductance L_e, and real part of the antenna impedance ReZ_e connected in series (figure 3(a)). Here L_e is determined by the slope of ImZ:

$$L_e = \frac{1}{4\pi} \frac{dImZ}{df} \qquad (1)$$

at the frequency of series resonance f_s ($ImZ = 0$, $f_s \sim$ 73.5 GHz for 75 GHz channel and $f_s \sim 102.4$ GHz for 105 GHz channel, see figure 2(b)). $L_e = 1.49 \times 10^{-9} H$ for 75 GHz and $L_e = 0.72 \times 10^{-9} H$ for 105 GHz.
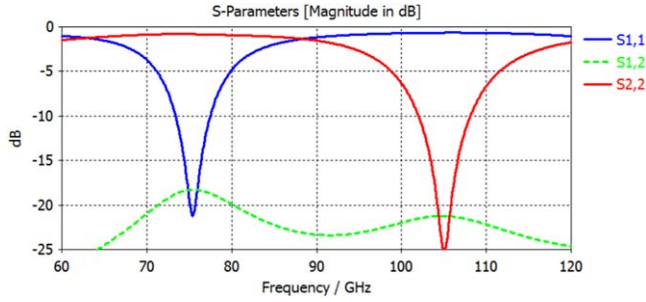
Figure 4. Frequency characteristics of the seashell antenna with CEBs tuned to 75 and 105 GHz.

At resonance frequency

$$C_e = \frac{1}{4 \cdot \pi^2 f^2 L_e}, \tag{2}$$

where $C_e = 3.02 \times 10^{-15}$ F for 75 GHz and 3.19×10^{-15} F for 105 GHz. It is essential that the operating frequencies $f_0 = 75$ or 105 GHz lie to the right of the corresponding frequencies of series resonances f_s, so that $\mathrm{Im}Z(f_0) > 0$.

The values of R_{abs} and C_{SIN} are chosen in the following way: $R_{abs} = \mathrm{Re}Z(f_0)$, $C_{SIN} = (2\pi f_0 \mathrm{Im}Z(f_0))^{-1}$, where $Z(f)$ is the diagonal component of the Z-matrix calculated in electrodynamics (see above). Here C_{sin} is chosen so that the total capacitance of C_{sin} and C_e forms the series resonance with L_e at operating frequencies 75 and 105 GHz, respectively. We note that such a way of parameter choice is valid only when $\mathrm{Im}Z(f_0) > 0$ and when $|S_{mn}(f_0)| \ll 1$, where S_{mn} are the nondiagonal components of the S-matrix calculated in electrodynamics. These components are actually the cross-talks between two-frequency channels of the antenna, and thus, they should be low. We also note that in such an approach the values of R_{abs} and C_{SIN} are defined uniquely.

As a result, spectral characteristics of the seashell antenna with two CEBs are obtained (figure 4). The values of R_{abs} and C_{SIN} are the following: for 75 GHz channel $R_{abs} = 54.1$ Ohm, $C_{SIN} = 77$ fF, for 105 GHz channel $R_{abs} = 43.7$ Ohm, $C_{SIN} = 67$ fF. The quality factors of these resonances can be found by

$$Q = \frac{2\pi f \cdot L_e}{\mathrm{Re}Z + R_{abs}} \tag{3}$$

and determine the bandwidths of the frequency channels.

From figure 4 one can see that the widths of the resonances are nearly 15 GHz for 75 GHz channel and 20 GHz for 105 GHz channel. These values meet the ESA requirements for the receiving system of the COrE project. The maximal cross-talk of the antenna -15 dB is reached around 75 GHz (shown by the green dashed curve in figure 4). There are parasitic resonances at frequency above 120 GHz in 75 GHz channel and frequency below 60 GHz in 105 GHz channel.

4. Experimental setup and measurements

Samples of a seashell antenna with coplanars and CEBs were fabricated by combining optical and electron-beam lithography, and a shadow evaporation technique. SEM
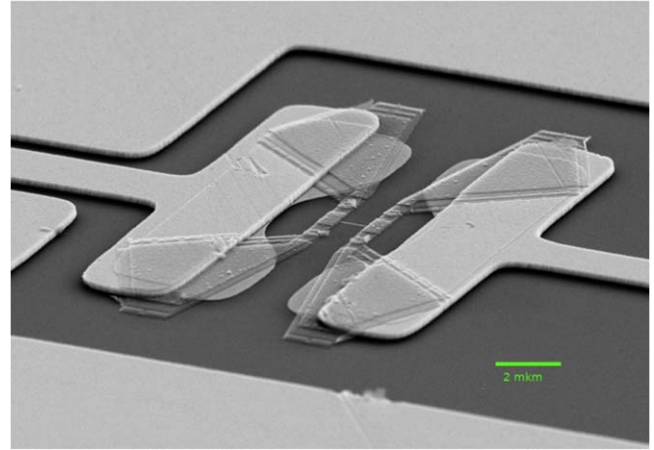

Figure 5. SEM image of the structure with CEBs embedded into the coplanar line.
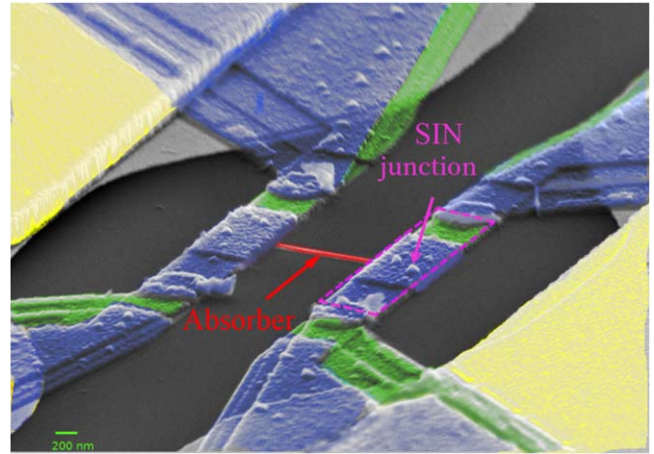

Figure 6. SEM image of the CEB comprising two SIN tunnel junctions and an absorber (red), first electrode—green, second electrode—blue, thin Au traps—grey, and gold antenna—yellow.

images of the structures are shown in figures 5, 6. Figure 5 shows the structure including CEB and normal metal traps for hot electrons embedded into the gap of the coplanar line. Figure 6 shows the detailed picture of a CEB with normal metal traps and Au antenna. For fabrication, first, a thin layer of gold of a thickness of 15 nm with titanium sublayer of 1 nm is deposited to create DC wires, then a SiO_2 dielectric layer of a thickness of 40 nm is deposited to separate the DC wires and the ground plane. Next, a ground plane layer of 130 nm gold and 20 nm palladium with a sublayer of 10 nm titanium is created. After these stages, a bolometric structure is fabricated using electron-beam lithography and self-aligned shadow evaporation technique. First, at 90° angle, evaporation of aluminum is done with the thickness of 14 nm with an iron sublayer of the thickness of 1.2 nm. Then, aluminum is oxidized at the pressure of 10 Torr for 5 min After oxidation, shadow evaporation of aluminum is performed at angles $+45°$ (first electrode, green color in figure 6) with a thickness of 40 nm, and $-45°$ (second electrode, blue color in figure 6) with a thickness of 50 nm.
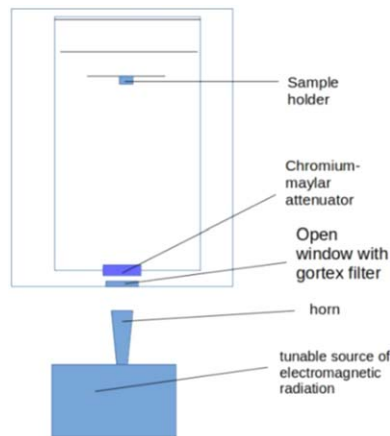
Figure 7. The setup of the experiment for measuring spectral characteristics.

Figure 8. Current–voltage characteristics of the sample without microwave irradiation from a calibrated BWO source and with radiation at frequencies 80, 85, 90, 95, 100, 105, 110, 115, 118 GHz. The response is calculated according to these characteristics. The largest response is observed at 105 and 110 GHz.

The sample placed in the holder has been attached to the center of the lower plate (300 mK) of the cryostat above the open window, through which radiation from an external source of electromagnetic radiation was fed. Figure 7 shows the arrangement of a cryostat with a sample and a radiation source. The source of radiation was a synthesizer based on a backward-wave oscillator (BWO), tunable in the range of 78–118 GHz.

During the experiment, the current–voltage characteristics of the sample structures were measured in the absence of an external signal [12, 13]. Then a tunable radiation source at frequency of 80 GHz was switched on, and the *I–V* characteristics of the structures were measured compared with the *I–V* characteristic with the switched off source. The structures having the most 'hot' *I–V* characteristics were subjected to additional investigation in the time-domain mode with a frequency sweep. In the frequency sweep, an external bias current, corresponding to the largest CEB voltage response had been applied to the structures.

Measurements in the time-domain mode were carried out in two-channel mode, so that it was possible to measure the response of the structures with resonances at 75 and 105 GHz during the frequency sweep, simultaneously. Such measurement of the response at two-frequency channels at the same time makes it possible to avoid the error associated with inaccurate matching between the measurement time and the frequency of the external oscillator.

5. Measurement results

The frequency response of the samples has been studied by irradiating them with a tunable source of electromagnetic radiation. In figure 8 one can see the current–voltage characteristics of the sample without microwave irradiation from a BWO synthesizer and with radiation at frequencies 80, 85, 90, 95, 100, 105, 110, 115, 118 GHz and the response on these frequencies. The response is the difference between current–voltage characteristic of the sample without radiation and current–voltage characteristic of sample with radiation. The
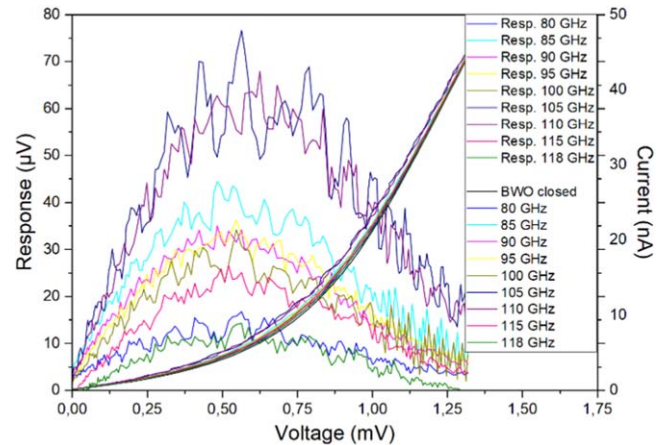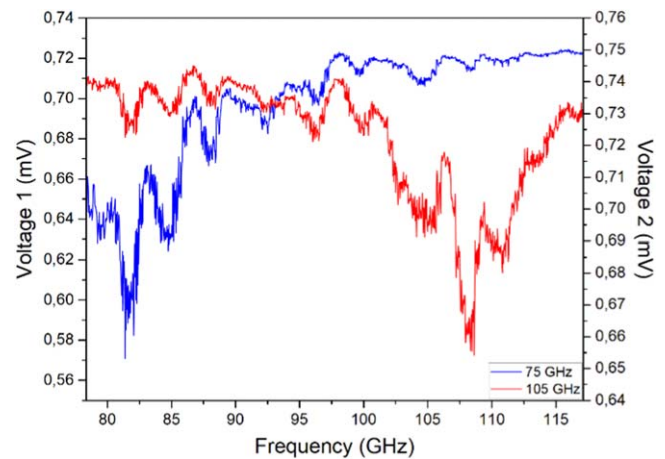

Figure 9. The response of the seashell antenna with CEBs to the external electromagnetic radiation, measured simultaneously in two-channel mode.

largest response is observed at 105 and 110 GHz, while at other frequencies the response decreases. In figure 9 the measured voltage during fast automatic frequency sweep of the BWO synthesizer is presented. Two samples designed for different frequencies are measured simultaneously in the two-channel mode to suppress possible external interference.

Figure 10 shows the frequency response of the sample of the seashell antenna (solid curves), the blue curve shows the resonance corresponding to the 75 GHz channel, the red curve —105 GHz channel. In comparison with figure 9 the curves are inverted and normalized to unity for more efficient comparison with theory. The blue and red dashed curves show the results of theoretical modeling, by which the samples have been fabricated. One can see good qualitative agreement between theory and experiment. However, the measured resonant frequencies are somewhat higher, and additional maxima due to standing waves inside cryostat are clearly visible. Certain disagreement in central frequencies and bandwidths may be due to a mismatch in the the oxidation of
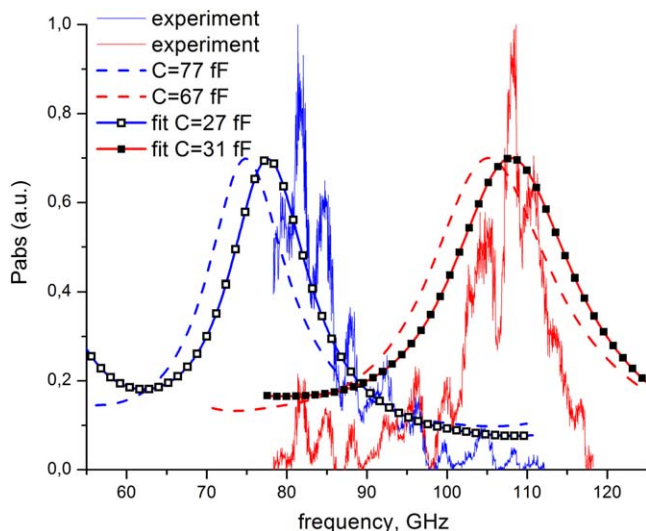
Figure 10. The measured response of the seashell antenna with CEBs to the external electromagnetic radiation (solid curves) compared to theoretical results corresponding to sample design (dashed curves) and to the fitting with the corrected SIN junctions capacitance and absorber resistance (solid curves with symbols).

aluminum in the fabrication of the bolometric structure, since the capacitances of the SIN junctions change.

Varying the system parameters one can perform the fitting of experimental data trying to understand the reason of the resonant frequency mismatch. Changing the CEB capacitance from 77 to 27 fF for 75 GHz channel and also resistance from 44 to 46 Ohm and capacitance from 67 to 31 fF for 105 GHz channel allows the resonant frequencies to be matched better (figure 10, solid curves with symbols). These results will be taken into account in the future designs, in order to make corrections to the technological process of the sample fabrication.

6. Conclusions

We have successfully demonstrated the operation of a novel multichroic seashell antenna with internal bandpass filters by resonant slots and CEB. The internal resonance is organized by a series resonance of slots with CPW and capacitances of SIN (superconductor/insulator/normal) tunnel junctions. This structure gives the opportunity to keep the size of the antenna just proportional to λ contrary to a conventional multichroic sinuous antenna and TESs connected by long microstrip lines with unavoidable losses, overlaps and external filters. Besides that, the seashell antenna gives an important opportunity to keep the beam width of the same size for different frequency bands due to the independent tuning of a beam by the corresponding pair of phased slots for each frequency channel.

With proper design of the antenna, we have elaborated and fabricated samples of the receiving system at two frequencies of 75 and 105 GHz. The results of measurements of these samples qualitatively agree with the results obtained by numerical modeling in the CST package. Slight disagreement

in central frequencies and bandwidths may be due to changes in the SIN junctions' capacitances and absorber resistances at the stage of lithography. The main advantage of the developed technology is the absence of additional niobium nitride layer for fabrication of kinetic inductance that significantly simplifies the fabrication process, and makes the system more reliable and less sensitive to the process of fabrication. Slots and CEBs are connected by CPW instead of microstrip lines to realize the most reliable single-layer technology with the only ground plane instead of three-layer technology for microstrip lines.

These experiments confirm that the seashell antenna with the internal filters by resonant slots and CEBs demonstrate considerable simplification of the structure with independent tuning for each frequency band and significant simplification of the technology. The multichroic seashell antenna can be effectively used for creating multiband elements for CMB polarimetry.

ORCID iDs

L S Kuzmin https://orcid.org/0000-0002-8051-484X
A L Pankratov https://orcid.org/0000-0003-2661-2745
A V Chiginev https://orcid.org/0000-0002-6676-9141

References

[1] Masi S *et al* 2008 *Mem. Soc. Ital.* **79** 887
[2] O'Brient R *et al* 2013 *Appl. Phys. Lett.* **102** 063506
[3] Trappe N *et al* 2016 *Proc. SPIE* **9914** 991412
[4] Kuzmin L 2002 *International Workshop on Superconducting Nano-Electronics Devices* ed J Pekola, B Ruggiero and P Silvestrini (Boston, MA: Springer) pp 145–54
[5] Kuzmin L 2008 *J. Phys.: Conf. Ser.* **97** 012310
[6] Tarasov M A, Kuzmin L S, Edelman V S, Mahashabde S and de Bernardis P 2011 *IEEE Trans. Appl. Supercond.* **21** 3635
[7] Salatino M, de Bernardis P, Kuzmin L S, Mahashabde S and Masi S 2014 *J. Low Temp. Phys.* **176** 323

[8] Kuzmin L S 2014 *IEEE Trans. THz Sci. Technol.* **4** 314–20

[9] Kuzmin L S, Mukhin A S and Chiginev A V 2018 *IEEE Trans. Appl. Supercond.* **28** 2400304

[10] Kuzmin L S, Chiginev A V, Matrozova E A and Sobolev A S 2016 *IEEE Trans. Appl. Supercond.* **26** 2300206

[11] Cukierman A, Lee A T, Raum C, Suzuki A and Westbrook B 2018 *Appl. Phys. Lett.* **112** 132601

[12] Gordeeva A V, Zbrozhek V O, Pankratov A L, Revin L S, Shamporov V A, Gunbina A A and Kuzmin L S 2017 *Appl. Phys. Lett.* **110** 162603

[13] Kuzmin L S, Pankratov A L, Gordeeva A V, Zbrozhek V O, Revin L S, Shamporov V A, Gunbina A A, Masi S and de Bernardis P 2017 *IEEE Xplore Proc. 16th Int. Superconductive Electronics Conf. (ISEC'2017)* (https://doi.org/10.1109/ISEC.2017.8314194)